

# Power Quality Disturbances (PQDs) Classification Analyzed Based on Deep Learning Technique

Ahsan Ali Memon<sup>1\*</sup>, Suhail khokhar<sup>1</sup>, Irfan Ali Channa<sup>2</sup>, Imdad Ali<sup>3</sup>, Sheeraz Ahmed<sup>4</sup> and Asif Nawaz<sup>5</sup>

<sup>1</sup>Department of Electrical Engineering, Quaid-e-Awam University of Engineering, Science and Technology Nawabshah, 67450, Pakistan.

<sup>2</sup>Department of Automation, Beijing University of Chemical Technology, Beijing, 100020, China.

<sup>3</sup>Department of Mechanical Engineering, Quaid-e-Awam University of Engineering, Science and Technology Nawabshah, 67450, Pakistan.

<sup>4</sup>Career Dynamics Research Center, Peshawar, Pakistan.

<sup>5</sup>Electrical Engineering Division, Higher Colleges of Technology, Dubai, 25026, UAE.

\*Corresponding Author: Ahsan Ali Memon. Email: ahsanmemon.444@gmail.com.

Received: September 21, 2022 Accepted: November 12, 2022 Published: December 29, 2022.

**Abstract:** Power Quality (PQ) problems in a distributed generation are mainly appeared due to excess non-linear load in the system. Identification and classification are necessary to ensure the reliability of Power Quality Disturbances (PQDs). This study proposed a signal processing and deep learning approach classify the PQDs by applying Discrete Wavelet Transform (DWT), Multi-Resolution Analysis (MRA) and a one-dimensional Convolutional Neural Network (CNN). For speed up in training, the performance of model a signal processing-based DWT-MRA extracted 54 features and fed it into 1D-CNN. Implementation of 1D-CNN seems more reliable than other machine learning approaches. Simulation results showed good performance and classification of data efficiently. Hence, the proposed approach could open a new era for PQDs in PV/wind smart grid in the near future to obtain more efficient outcomes.

**Keywords:** DWT; MRA; Deep learning; CNN; Power Quality Disturbance.

## 1. Introduction

Recently, clean power has gained more attention because the technology has advanced, and so have consumer energy demands and the use of complicated loads. Hybrid energy systems are now used more frequently as a result of the inadequacy of local energy producing methods. PQDs are highlighted as the directed for the power system constraints like frequency, voltage and current (Eristi & Eristi, 2022b). PQDs are an important issue for both power utilisation and consumers due to the low losses produced by modern power electronics equipment, heavy non-linear loads, rectifiers, and inverters. Identifying PQDs in a Renewable Micro Grid is essential for defining the system's decision-making method and proper operation. Identification of PQDs consists of two types of stages; such as feature extraction and classification. Therefore, the feature extraction level extracts distinctive features of data. Suppose the data is perfect and gets a high performance, the classification level reorganisation of more output. To analyse PQDs, many signal-processing methods could be proposed (Zhang et al., 2003). The theorems such as Short-Time Fourier Transforms, Hilbert-Huang transform, Kalman filter (KF), Wavelet Transform (WT), S-Transform (ST), Fast Fourier transform (FFT), and Curvelet Transform (CT) are applied in PQDs feature extraction (Eristi & Eristi, 2022b; Jamali et al., 2018; Liu, Hussain, & Shen, 2018; Shen et al., 2018).

The classification phase determined the kinds of PQDs by the feature extraction phase analysis. For the PQDs classification, feature extraction was recognised by Artificial Neural Networks (ANN) before the 2000s. Still, other methods, including a k-nearest neighbour, fuzzy expert systems, support vector machines

(SVM) and genetic method, were established to classify intelligent mechanisms and dramatically used for the PQDs classification stage. Nowadays, the most popular classifiers used are Deep Learning Based, an intelligent image reorganisation algorithms approach to recognise systems for PQDs (Ekici et al., 2021; Liu et al., 2019; Liu, Hussain, Shen, et al., 2018; Wang & Chen, 2019).

Recently, many researchers focused on power systems because the significant implementation of the Solar Photo Voltaic (SPV) scheme is increased in the power field. In a later study survey, power integrated with SPV had a negative impact on the power system. The performance of traditional methods versus Artificial Intelligence (AI) systems for justifying PQDs. From the obtained result, it was emphasised that AI systems' controlling and response time is significantly higher than traditional methods (Chawda et al., 2020). Therefore, fuzzy c-means (FCM) and ST congregation algorithm has been offered in PQDs integrated along SPV through the power system. Furthermore, the reported study discussed ST-based techniques for PQDs sensing, islanding, interruption, and grid synchronisation with renewable energy sources in a power system. Therefore, a SVM, WT and independent component method for PQDs detection in a SPV micro grid (Ray et al., 2019).

PQ problems are brought by non-linear electronic loads and distributed generations that are connected to the grid. Fluctuations and loads affect the signal's capacity, leading to non-stationary PQDs. PQDs can be brought on by abrupt changes in frequency, amplitude, current, and phase angle. This problem has been resolved using DWT and MRA-based CNN algorithms for automatic categorisation and detection of PQDs. A PQD signal's feature extraction yields information that aids in PQD detection. Power engineers may more effectively monitor and maintain power disturbances with the help of an accurate and efficient feature extraction tool.

## 2. Methodology

In this section, Power Quality Disturbances, Feature extraction using Statistical Parameters and AlexNet are discussed. , However, the Discrete Wavelet Transform, Multi-Resolution Analysis and Deep Learning techniques are introduced for the classification of PQDs.

### 2.1 Power Quality Disturbances

The proposed algorithms have been accessed for the classification performance using Ten (10) types of parametric equations of PQDs signals and

Pure sine wave, Normal, Sag, Swell, Interruption, Harmonics, Flicker, as well as Oscillatory Transients are the seven single types seen in PQDs, respectively. In addition, Sag with harmonics, swell with harmonics, and interruption with harmonics are the three kinds of PQDs. Furthermore, the table.1 displays parametric equations in accordance with IEEE-1159 standard [6] with parametric variations. Additionally, the typical PQ waveforms by applying a characteristics equation as given below in Figure 1.

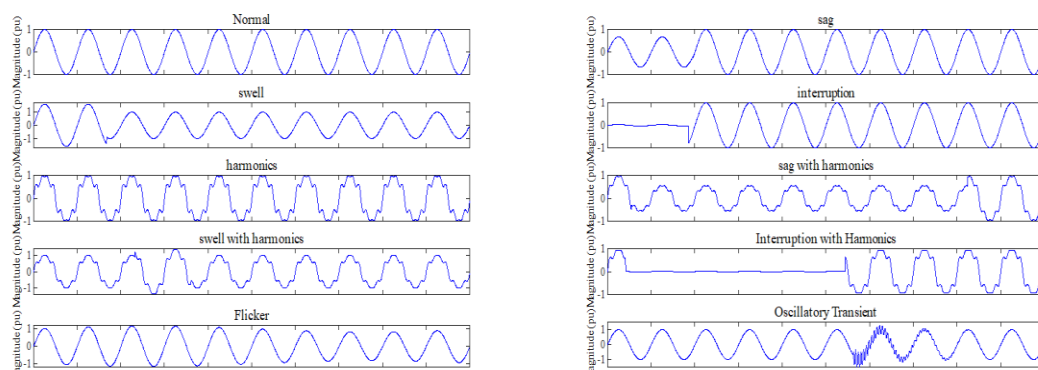


**Figure 1.** Parametric waveform of PQDs

The waveforms of parametric frequency are 6 kHz with 10 cycles were developed for a maximum of 2000 sampling points. The parameter A is fixed (1 per unit) in all PQDs parametric equations representing waveform amplitude. The parameters indicate the strength of swell, interruption and sag, which possesses variations concerning the type of disturbances. The time duration of disturbance can be provided by the

step function in a pure sine waveform. Waveforms of 10 cycles are produced using 2000 sampling points at a sampling frequency of 6 kHz in the overall parametric equations in the PQDs. The A denotes the amplitude of the waveform as well as a constant value (1 per unit). Additionally, depending on the type of disturbances, the parameter varies the strength of the sag, swell, and interruption. In a pure waveform, the step function controls the duration of the disturbance. The 3rd, 5th, and 7th harmonics, whose per-unit values vary from 0.05 to 0.15 of the basic magnitude into the total useful combination, are responsible for harmonic disturbances. Similarly, disturbances caused by swell, interruption, and sag give various PQDs a combination of harmonic disturbances. In a flicker,  $\beta$  denotes a flicker frequency range of 5 to 20 Hz, and  $\alpha_f$  denotes 0.1 to 0.2 per unit flicker disturbance magnitude range. Transient frequency  $f_n$  in oscillatory transient ranges from 300 to 900 Hz, while Transient time constant  $\tau$  is between 0.008 and 0.04 seconds. The size of the impulsive transient is indicated by  $\alpha_i$  and ranges from 0 to 0.414 per unit. However, the width varies between 0.01 cycle and 0.05 cycle, while the size of the spike and notch varies between 0.1 and 0.4 per unit, according to the K parameter (Liu, Hussain, Shen, et al., 2018)(Ray et al., 2019).

In several aspects, the PQDs created by using parametric equations have been proved useful. The disturbances attracted a lot of attention and can be easily recognised by behaviour. Therefore, it has the potential to deliver the proper training and testing data set parameters in a variety of controlled ways. Meanwhile, to approach the generating capability of the classifier, the addition of the associated signals offers the possibility of the same class.

**Table 1.** Mathematical Models of single and Multiple PQDs (Khokhar et al., 2017).

Label	PQD	Mathematical equations	parameters
C1	Normal	$y(t) = A[1 \pm \alpha(u(t-t_1) - u(t-t_2))] \sin(\omega t)$	$\alpha \leq 0.1; T \leq t_2 - t_1 \leq 9T$
C2	Sag	$y(t) = A[1 - \alpha(u(t-t_1) - u(t-t_2))] \sin(\omega t)$	$0.1 \leq \alpha \leq 0.9; T \leq t_2 - t_1 \leq 9T$
C3	Swell	$y(t) = A[1 + \alpha(u(t-t_1) - u(t-t_2))] \sin(\omega t)$	$0.1 \leq \alpha \leq .8; T \leq t_2 - t_1 \leq 9T$
C4	Interruption	$y(t) = A[1 - \alpha(u(t-t_1) - u(t-t_2))] \sin(\omega t)$	$0.9 \leq \alpha \leq 1; T \leq t_2 - t_1 \leq 9T$
C5	Harmonics	$y(t) = A[\alpha_1 \sin(\omega t) + \alpha_3 \sin(3\omega t) + \alpha_5 \sin(5\omega t) + \alpha_7 \sin(7\omega t)]$	$0.05 \leq \alpha_3, \alpha_5, \alpha_7 \leq 0.15; \sum \alpha_i^2 = 1$
C6	Sag with harmonics	$y(t) = A[1 - \alpha(u(t-t_1) - u(t-t_2))] [\alpha_1 \sin(\omega t) + \alpha_3 \sin(3\omega t) + \alpha_5 \sin(5\omega t)]$	$0.1 \leq \alpha \leq 0.9; T \leq t_2 - t_1 \leq 9T$ $0.05 \leq \alpha_3, \alpha_5, \alpha_7 \leq 0.15; \sum \alpha_i^2 = 1$
C7	Swell with harmonics	$y(t) = A[1 + \alpha(u(t-t_1) - u(t-t_2))] [\alpha_1 \sin(\omega t) + \alpha_3 \sin(3\omega t) + \alpha_5 \sin(5\omega t)]$	$0.1 \leq \alpha \leq 0.8; T \leq t_2 - t_1 \leq 9T$ $0.05 \leq \alpha_3, \alpha_5, \alpha_7 \leq 0.15; \sum \alpha_i^2 = 1$
C8	Interruption with harmonics	$y(t) = A[1 - \alpha(u(t-t_1) - u(t-t_2))] [\alpha_1 \sin(\omega t) + \alpha_3 \sin(3\omega t) + \alpha_5 \sin(5\omega t)]$	$0.9 \leq \alpha \leq 1; T \leq t_2 - t_1 \leq 9T$ $0.05 \leq \alpha_3, \alpha_5, \alpha_7 \leq 0.15; \sum \alpha_i^2 = 1$
C9	Fliker	$y(t) = A[1 + \alpha_f \sin(\beta \omega t)] \sin(\omega t)$	$0.1 \leq \alpha_f \leq 0.2; 5 \leq \beta \leq 20Hz;$
C10	Oscillatory transient	$y(t) = A \left[ \sin(\omega t) + \alpha \frac{-c(t-t_1)}{\tau} \sin \omega_n(t-t_1)(u(t_2) - u(t_1)) \right]$	$0.1 \leq \alpha \leq 0.08; 0.5t \leq t_2 - t_1 \leq 3T$ $8ms \leq \tau \leq 40ms; 300 \leq f_n \leq 900Hz$

## 2.2 Discrete Wavelet Transform

It examines the local discontinuities in the signal, the Wavelet Transform (WT) is used to study non-stationary and steady-state signals in a variety of domains. Therefore, PQDs in power systems are non-stationary transients, and the usage of WT in PQ works was noted and observed as being of extremely high significance. The mathematical CWT of a continuous signal w.r.t the wavelet function is mentioned below.

$$CWT(a, b) = \frac{1}{\sqrt{a}} \int_{-a}^a f(t) \psi \left( \frac{t-b}{a} \right) dt \quad a, b \in R, \quad a \neq 0 \quad (1)$$

The constant, translation constraints and stand for the measurement are, respectively, in fig 1. The length of the wavelet and oscillation frequency is provided by the parameter scale. Furthermore, the translation parameters deposit their fluctuating site. Therefore, the sequence of wavelet factors is the output at each gauge that denotes the whole transient signal. CWT will be redundant for computer analysis with the information appropriate for practical applications. So, in equation 2, DWT was noted as more reliable for investigating the PQDs system.

$$DWT(m,n) = \frac{1}{\sqrt{a_0^m}} \sum f(k) \psi\left(\frac{n - kb_0 a_0^m}{a_0^m}\right) \tag{2}$$

The translation and scaling constraints are substituted by  $m$  and  $n$  integer functions, i.e.,  $a = a_0^m$  and  $b = kb_0 a_0^m$ , correspondingly, although  $f(k)$  is a collection of discrete points from the continuous time signal  $f(t)$ . A proper mother wavelet is essential for investigating the results, and it consists of the category of data used from the selection of the WT application. The mother wavelets are examined in the PQ analysis, namely, Mexican, Haar, Bi-orthogonal, Morlet and Daubechies (Erişti et al., 2013).

### 2.3 Multi-Resolution Analysis:

The most crucial method utilised for the reconstruction and decomposition of signals at various resolution levels is called Multi-Resolution Analysis (MRA). Decomposing of PQDs waveforms MRA theory is always applied because it is a very easy technique with low memory usage. MRA represents the signals at different resolution stages. For reconstructing and decomposing the signals at various resolution limits, building blocks include the scaling function  $\varphi_{m,n}(t)$  and orthogonal wavelet  $\psi_{m,n}(t)$ . For Example, High-Pass (HP) and Low-Pass (LP) filters pass a time-domain signal  $f(t)$  from two filters at each step. So, HP filters provide the high-frequency components recognised as aspect coefficient (D1), while LP provides the low-frequency features of the original time-domain signal approximation coefficient (A1). LP and HP have the same frequency band, and the sampling frequency is classified into two after each decomposition cycle (Khokhar et al., 2017). Then LP filter (A1) output is decomposed continually. However, the two components (D2) and (A2) of the next stage are developed and mentioned in figure 2. Therefore, the whole mechanism up to desired decomposition level is repeated (Dehghani et al., 2013).

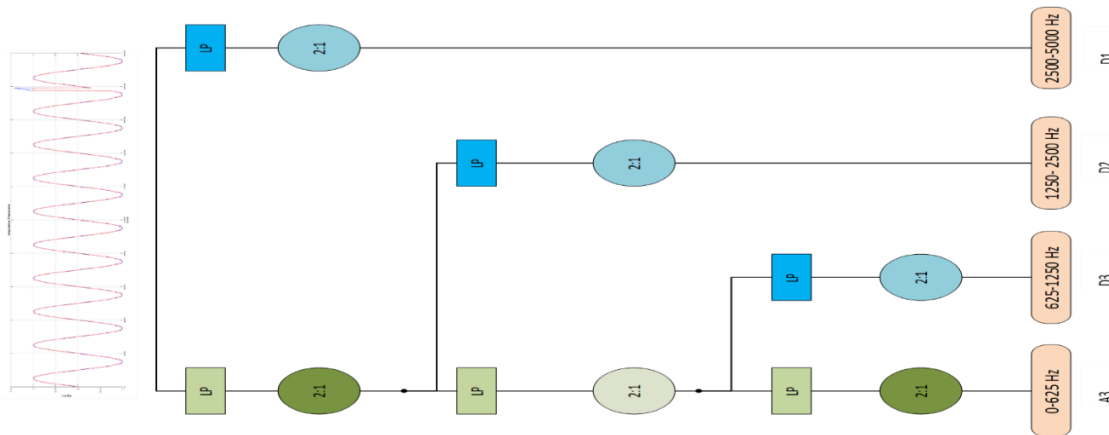


Figure. 2 Multi-Resolution Analysis

It is possible to express the signal  $f(t)$  decomposition into approximations and specifics by scaling  $\varphi_{m,n}(t)$  and wavelet  $\psi_{m,n}(t)$  as stated in equations (3) and (4)

$$\varphi_{m,n}(t) = 2^{\left(\frac{-m}{2}\right)} \varphi\left(2^{-m}t - n\right) \tag{3}$$

$$\psi_{m,n}(t) = 2^{\left(\frac{-m}{2}\right)} \psi\left(2^{-m}t - n\right) \tag{4}$$

Wavelet and scaling functions are connected to HP and LP filters. The decomposition method starts with the passing of signals using filters. At the instant  $k$  to  $j$  scale, the decomposition of a discrete signal  $f(p)$  and WT based on MRA yields low and high-frequency coefficients  $D_j(p)$  and  $A_j(p)$ . Generally, the total parameters mentioned below can be used to represent the input signal  $f(p)$ .

$$\begin{aligned}
f(k) &= D_1(p) + A_1(p) \\
&= D_1(p) + D_2(p) + A_2(p) \\
&= D_1(p) + D_2(p) + D_3(p) + A_3(p) \\
&= \sum_{j=1}^l D_j(p) + A_l(p)
\end{aligned}$$

Where  $j=1,2,\dots, 6$  denotes the stage of the wavelet decomposition. So feature vector size in signal  $f(p)$  is length  $L+1$  equation 5.

$$f(p) = [D_1, D_2, \dots, D_l, A_l] \quad (5)$$

For a pure sine wave, harmonics, sag, and notch disturbance waveforms, Fig.2 represents the approximation plot of level 6 and detailed level 1 to 6 DWT. Waveforms decomposition specifies PQDs discretely from where type and disturbance period could be significantly recognised. Due to the smooth pure sine waveform, no vibration is indicated (Khokhar et al., 2017).

#### 2.4 Feature extraction using Statistical Parameters

The statistical components used in feature extraction are found in previous research work. The mathematical equation shown in table II [15] can be used to compute the five statistical parameters known as Energy (E), Entropy (Ent), Standard Deviation ( $\sigma$ ), Mean Value ( $\mu$ ), Root Mean Square (RMS), and Range Value (RG) of approximation (A) and detail (D) coefficients. (Singh & Singh, 2019).

**Table 2.** Statistical parameters (Khokhar et al., 2017)

Statistical Parameters Equation	
Energy	$E_i = \sum_{j=1}^N ( A_{ij} ^2,  D_{ij} ^2)$
Entropy	$Ent = -\sum_{j=1}^N \{A_{ij}^2 \log(A_{ij}^2), D_{ij}^2 \log(D_{ij}^2)\}$
Standard deviation	$\sigma_i = \left( \frac{1}{N-1} \sum_{j=1}^N \{(A_{ij} - \mu_i)^2, (D_{ij} - \mu_i)^2\} \right)^{1/2}$
Mean	$\mu_i = \frac{1}{N} \sum_{j=1}^N (A_{ij}, D_{ij})$
RMS Value	$RMS_i = \left( \frac{1}{N} \sum_{j=1}^N (A_{ij}^2), (D_{ij}^2) \right)^{1/2}$
Range	$RG_i = Max(A_{ij}, D_{ij}) - Min(A_{ij}, D_{ij})$

Here  $i = 1, 2, \dots, 6$  denotes the total number of wavelet decompositions at stage  $l$ , and  $N$  represents the number of coefficients in each decomposed data.

PQDs waveforms are divided into six stages for the predicted feature selection technique that provides six feature coefficients ( $D_1, D_2, \dots, D_6$ ) and an approximation coefficient ( $A_6$ ). The total feature of approximation and detail coefficients are obtained 54, from which the finest features were chosen, providing high classification accuracy. The statistical feature vector is below,

$$\begin{aligned}
F_1 &= [E_{D1} E_{D2} \dots E_{D6} E_{D6}], \\
F_2 &= [Ent_{D1} Ent_{D2} \dots Ent_{D6} Ent_{D6}]; \\
F_3 &= [\sigma_{D1} \sigma_{D2} \dots \sigma_{D6} \sigma_{D6}]; \\
F_4 &= [\mu_{D1} \mu_{D2} \dots \mu_{D6} \mu_{D6}]; \\
F_5 &= [RMS_{D1} RMS_{D2} \dots RMS_{D6} RMS_{D6}] \\
F_6 &= [RG_{D1} RG_{D2} \dots RG_{D6} RG_{D6}]
\end{aligned}$$

F1, F2, F3, ..., F6 signifies the main features vector of entropy, energy, standard deviation, mean, range values and RMS detailed coefficients and approximation values of DWT. Moreover, the whole data of ten types of the PQDs impacts the classifier's performance, which exists in the extensive feature set. So, the data should be standardised between 0 and 1. Keep in view that before getting input data to the classifier. In addition, features vector Utilising the min-max technique,  $F_i$  derived from MRA is normalised between 0 and 1 (Khokhar et al., 2017).

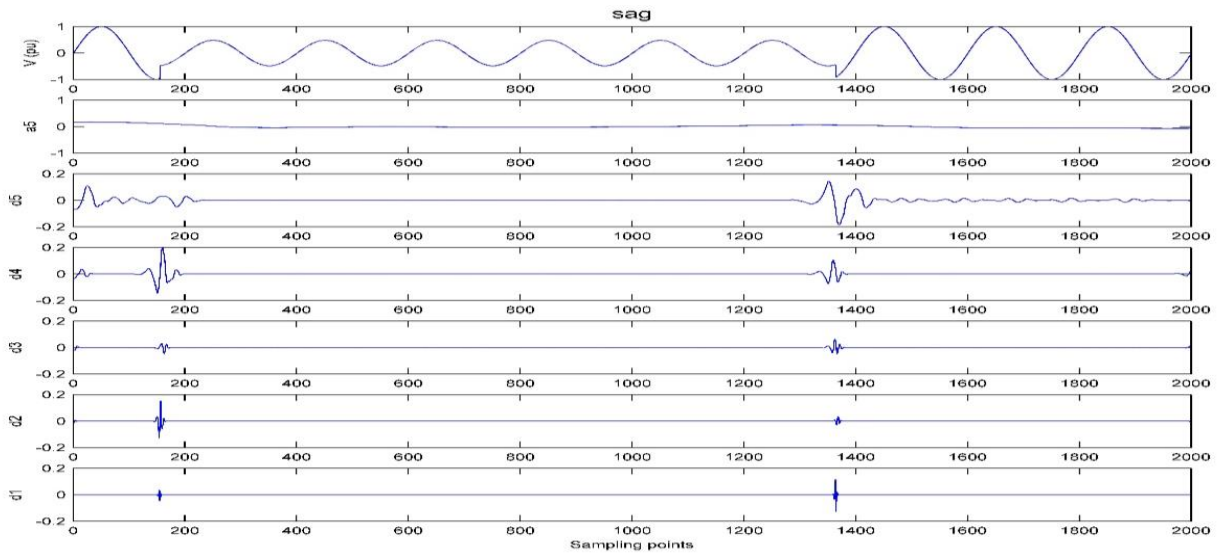


Figure 3. Wavelet coefficient of sag

$$Z_i = \frac{F_i - F_{\min}}{F_{\max} - F_{\min}} \quad (6)$$

Here  $Z_i$  denotes the standardised data,  $F_{\min}$  and  $F_{\max}$ , which are the feature vector  $F_i$  minimum and maximum data. Once the data have been normalised. Consequently, the entire feature set following data normalising is shown below in equation 7.

$$Feature = [F_1 F_2 F_3 F_4 F_5 F_6] \quad (7)$$

## 2.5 Deep Learning

In classifying PQDs, specific feature performances are highly significant for the classification domain. PQD was categorised using a Deep Convolutional Neural Network (DCNN)-based classifier, and dropouts were applied for overfitting the training. Recently, DCNNs were developed for spontaneously learning the features from selected considerations of the large-scale dataset and observing the remarkable output of the tool (Eristi & Eristi, 2022a).

### 2.5.1 AlexNet

The AlexNet Deep Convolutional Neural Network (DCNN) effectively processed 1.2 million photos from the ImageNet and 1000 samples of images as an anticipated culture structure had about 60 million factors and 650k neurons. This possessed around three fully connected layers. Further, there are three max-pooling layers, five convolutional layers, and two normalisation layers. Next, the last layer is labelled with 10-route classifier software that simplifies logistic deterioration for multi-classification. For the reduction of overfitting the data, the dropout method with the last layer is employed, and for the activation of fully connected layers and convolutional the Rectified Linear Units (ReLU) have been applied (Eristi & Eristi, 2022a; Hinton et al., 2012).

The dimensionality of the extracted feature plays the most important role in the classification domain for classifying PQDs. The feature selection method was carried out and applied to the training data during the algorithm's training phase. For the classification of PQD, a DCNN-based classifier is presented, and dropout is used to avoid overfitting the training. For automatically learning the feature from a huge dataset, DCNNs have been developed, and they have demonstrated notable performance in object identification. The classification accuracy and calculation speed of the DCNN are significantly improved. Given the increasing expansion of monitoring devices in multi-energy systems, it is appropriate for big data analysis of power quality disturbance data.

## 3. Results and Discussions

To appraise the employed method for the classification, 7 types of single and 3 complex PQDs with 2000 samples are to be considered. These PQDs are given in Table 1. Artificial single and complex PQDs waveforms are created on MATLAB R2021a through mathematical models.

These PQDs were designed randomly and per the recommended IEEE standard. PSCAD software was employed for the generation of PQD waveforms. The 6KV distribution network is designed and generates line faults containing single-line-ground, line-to-line, and double line-to-ground faults producing time domain waveforms known as swell, interruption and sag (Liu, Hussain, Shen, et al., 2018).

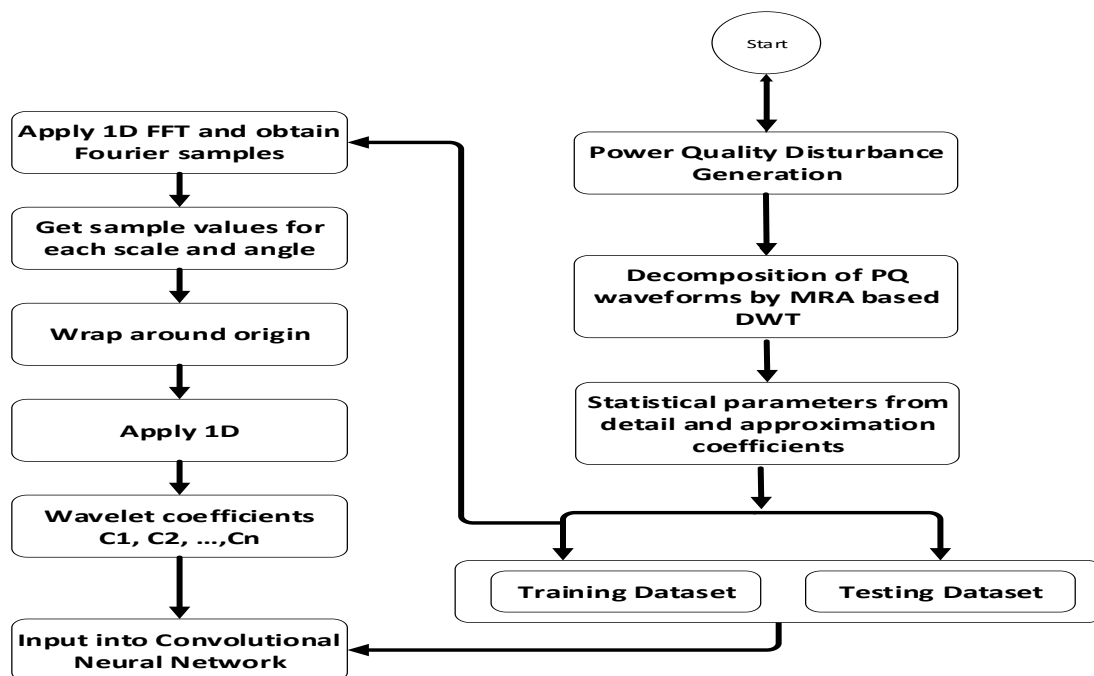


**Figure 4.** Flow chart of feature extraction and signal decomposition on DWT and MRA-based DCNN.

The two main steps of the methodology are classified as comprised of feature extraction from signals, and the intelligent system DCNN are applied for PQD classification. The PQD signals are decomposed by using DWT-MRA based DCNN methods. In the end, DWT-MRA based DCNN classifiers are applied to

classify PQDs signals. However, the experimental work was performed 50 times after validating the suggested method. In each execution, the dataset is classified into training and testing samples, 70% and 30%, correspondingly. For the detection and classification of PQD following procedure is adopted. PQD waveform classification is based on DWT-MRA based DCNN with input Single and Complex PQD signals (x).

STEP 1: Confusion Matrix  $X_{ij}^{N \times m}$  is produced using the input signal (x).

$$X_{ij} + X_{i+j-1}$$

Where  $1 \leq j \leq m$  and  $1 \leq I \leq N = N_t - m + 1$ . The whole data for the PQD signal was contained in the confused Matric, which occurred in a specific size m. however, specific sizes possibly varied.

Step 2: Furthermore, for feature selection, the DCNN algorithm is applied, and MRA and DWT classifiers are used to classify the PQD and label each section.

The employed feature extraction and classification algorithms (MRA-DWT based DCNN) are given in figure 5.

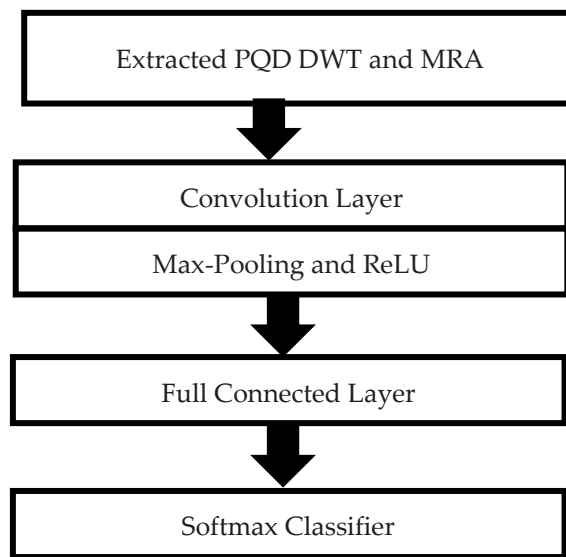


Figure 5. Classification flow chart of Algorithm (DWT-MRA based DCNN)

The proposed DWT-MRA based DCNN classifier around 2000 samples of 7 single and 3 complex PQD was conducted. It extracts the PQD through proposed algorithms, then sends it to the convolution layer and max pooling after passing from it. It goes to the final steps full connected layer and Softmax classifier, which classify the signals. For the selection of the best classifier, different techniques have been considered. DWT-MRA based DCNN classifier of 10 categories which gives the best result. From the results, DWT-MRA based DCNN classifier had significantly higher classification. figure 6 shows the DWT- MRA based DCNN classifier.

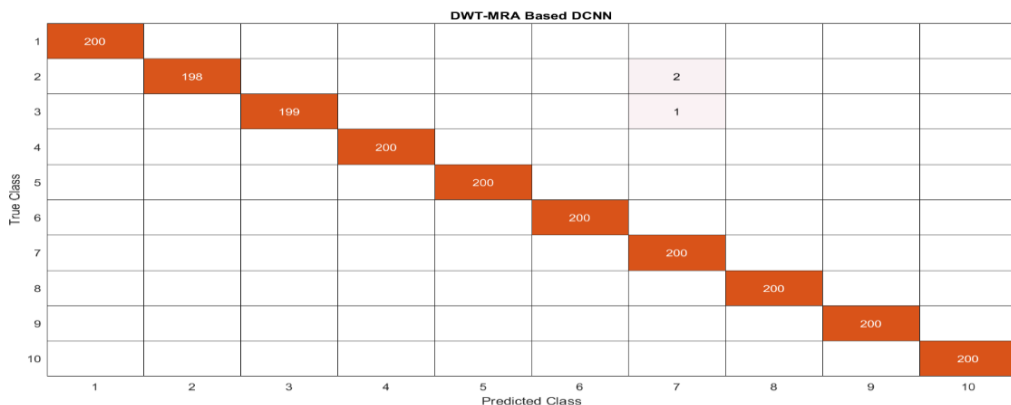


Figure 6. Confusion Matric for PQD classification

The DWT and MRA methods are applied to increase the classification rate of the PQD signals. Since there are ten different forms of PQDs, the observed result is 99.37%. Only complex and 110 samples are used in this method's verification for each PQD signal.

The fuzzy approach for the classification of around 98.71% with seven types of PQD was used in conjunction with DWT to extract feature characteristics. Eight different types of PQD were classified using the Fuzzy-ARTMAP wavelet neural network technique, with a 99.66% average classification accuracy. Moreover eleven single and twenty-one complex PQDs have been subjected to the rule-based classifier and sparse signal decomposition (SSD), yielding accuracy results of 99.87% and 96%, respectively (Liu, Hussain, Shen, et al., 2018) (Abdelsalam et al., 2012).

In order to capture multi-scale features and minimise overfitting, a unit structure made up of 1-D convolutional, pooling, and batch-normalization layers are created taking into account the properties of the power quality disturbances problem. Multiple units are stacked in the proposed DCNN to automatically extract features from large disturbance data. The disadvantages of traditional signal analysis and human feature selection may easily be overcome for the classification of PQDs because the implementation of deep learning can automatically realise the extraction, selection, and combination of PQDs features.

While other existing algorithms have a low categorisation rate, these methods have demonstrated good classification accuracy. However, most present techniques have been tested on single and complex PQD signals with sparse sample counts. The algorithm could be applied for analysis of PQD signals in real time. However, its time delay makes it better suited for offline applications. The MRA and DWT approaches are more dependable on the characteristics study of complicated transient (non-stationary) PQD signals.

**Table 3.** Results Comparison of various PQD classification methods

S. No	Technique	No. of Single PQDs	Result of Single PQDs (%)	Total complex PQDs	Result of total complex PQDs (%)
1	DCNN (Wang & Chen, 2019)	9	99.89	22	98.08
2	SSA + CT + DCNN (Liu, Hussain, Shen, et al., 2018)	9	100	22	99.52
3	Deep Learning (Ma et al., 2017)	5	99.65	2	100
4	Rule-based and SSD (Rupal et al., 2018)	11	99.87	21	96
5	SCICA (Ferreira et al., 2015)	5	-	12	97
6	HST, DWT (Hajian & Foroud, 2014)[29]	7	-	2	99.55
7	WT Fuzzy-ARTMAP	6	99.69	2	96
8	FES and DWT + KF (Decanini et al., 2011)	5	99	2	98
9	NN-MLP and ST (Decanini et al., 2011)	7	99.57	2	100
10	WNN (Uyar et al., 2008)	5	94.01	2	100
11	Current research work	7	99.37	3	99.37

#### 4. Conclusion and Future Work

An approach of feature extraction and one-dimensional CNN for classifying PQDs have been introduced. The proposed DWT-MRA and 1D-CNN have detected single and multiple types of PQDs. The 1D-CNN efficiently classifies data using features energy, entropy, skewness, STD, mean, RMS value and range.

Signal processing-based DWT-MRA measured the most common distinctive feature that supports the classifier. By applying artificial single and complex PQDs waveforms are observed. These PQDs were designed randomly as per the recommended IEEE standard. PSCAD/EMTDC software was employed for the generation of PQD waveforms. The 6KV distribution network is designed and generated line faults are created. Using MATLAB R2021a through mathematical models an accuracy was recorded at about 99.37%. In future work, validation can be checked with numerous aspects of power signals with real-world PQDs data. So, it can classify acceptable seven single and 3 complex PQD signals. Hence, these results suggested that the methods utilized in this study could be implemented for the identification and classification of simple and complex PQDs.

**References**

1. Abdelsalam, A. A., Eldesouky, A. A., & Sallam, A. A. (2012). Classification of power system disturbances using linear Kalman filter and fuzzy-expert system. *International Journal of Electrical Power and Energy Systems*, 43(1), 688–695. <https://doi.org/10.1016/j.ijepes.2012.05.052>
2. Chawda, G. S., Shaik, A. G., Shaik, M., Padmanaban, S., Holm-Nielsen, J. B., Mahela, O. P., & Kaliannan, P. (2020). Comprehensive Review on Detection and Classification of Power Quality Disturbances in Utility Grid with Renewable Energy Penetration. *IEEE Access*, 8, 146807–146830. <https://doi.org/10.1109/ACCESS.2020.3014732>
3. Decanini, J. G. M. S., Tonelli-Neto, M. S., Malange, F. C. V., & Minussi, C. R. (2011). Detection and classification of voltage disturbances using a Fuzzy-ARTMAP-wavelet network. *Electric Power Systems Research*, 81(12), 2057–2065. <https://doi.org/10.1016/j.epsr.2011.07.018>
4. Dehghani, H., Vahidi, B., Naghizadeh, R. A., & Hosseinian, S. H. (2013). Power quality disturbance classification using a statistical and wavelet-based Hidden Markov Model with Dempster-Shafer algorithm. *International Journal of Electrical Power and Energy Systems*, 47(1), 368–377. <https://doi.org/10.1016/j.ijepes.2012.11.005>
5. Ekici, S., Ucar, F., Dandil, B., & Arghandeh, R. (2021). Power quality event classification using optimized Bayesian convolutional neural networks. *Electrical Engineering*, 103(1), 67–77. <https://doi.org/10.1007/s00202-020-01066-8>
6. Eristi, B., & Eristi, H. (2022a). A new deep learning method for the classification of power quality disturbances in hybrid power system. *Electrical Engineering*. <https://doi.org/10.1007/s00202-022-01581-w>
7. Eristi, B., & Eristi, H. (2022b). Classification of Power Quality Disturbances in Solar PV Integrated Power System Based on a Hybrid Deep Learning Approach. *International Transactions on Electrical Energy Systems*, 2022, 11–14. <https://doi.org/10.1155/2022/8519379>
8. Erişti, H., Yildirim, Ö., Erişti, B., & Demir, Y. (2013). Optimal feature selection for classification of the power quality events using wavelet transform and least squares support vector machines. *International Journal of Electrical Power and Energy Systems*, 49(1), 95–103. <https://doi.org/10.1016/j.ijepes.2012.12.018>
9. Ferreira, D. D., Seixas, J. M. D., & Cerqueira, A. S. (2015). A method based on independent component analysis for single and multiple power quality disturbance classification. *Electric Power Systems Research*, 119, 425–431. <https://doi.org/10.1016/j.epsr.2014.10.028>
10. Hajian, M., & Foroud, A. A. (2014). A new hybrid pattern recognition scheme for automatic discrimination of power quality disturbances. *Measurement: Journal of the International Measurement Confederation*, 51(1), 265–280. <https://doi.org/10.1016/j.measurement.2014.02.017>
11. Hinton, G. E., Srivastava, N., Krizhevsky, A., Sutskever, I., & Salakhutdinov, R. R. (2012). Improving neural networks by preventing co-adaptation of feature detectors. 1–18. <http://arxiv.org/abs/1207.0580>
12. Jamali, S., Farsa, A. R., & Ghaffarzadeh, N. (2018). Identification of optimal features for fast and accurate classification of power quality disturbances. *Measurement: Journal of the International Measurement Confederation*, 116, 565–574. <https://doi.org/10.1016/j.measurement.2017.10.034>
13. Khokhar, S., Mohd Zin, A. A., Memon, A. P., & Mokhtar, A. S. (2017). A new optimal feature selection algorithm for classification of power quality disturbances using discrete wavelet transform and probabilistic neural network. *Measurement: Journal of the International Measurement Confederation*, 95, 246–259. <https://doi.org/10.1016/j.measurement.2016.10.013>
14. Liu, H., Hussain, F., & Shen, Y. (2018). Power Quality Disturbances Classification Using Compressive Sensing and Maximum Likelihood. *IETE Technical Review (Institution of Electronics and Telecommunication Engineers, India)*, 35(4), 359–368. <https://doi.org/10.1080/02564602.2017.1304290>
15. Liu, H., Hussain, F., Shen, Y., Arif, S., Nazir, A., & Abubakar, M. (2018). Complex power quality disturbances classification via curvelet transform and deep learning. *Electric Power Systems Research*, 163(May), 1–9. <https://doi.org/10.1016/j.epsr.2018.05.018>
16. Liu, H., Hussain, F., Shen, Y., Morales-Menendez, R., Abubakar, M., Junaid Yawar, S., & Arain, H. J. (2019). Signal Processing and Deep Learning Techniques for Power Quality Events Monitoring and Classification. *Electric Power Components and Systems*, 47(14–15), 1332–1348. <https://doi.org/10.1080/15325008.2019.1666178>
17. Ma, J., Zhang, J., Xiao, L., Chen, K., & Wu, J. (2017). Classification of Power Quality Disturbances via Deep Learning. *IETE Technical Review (Institution of Electronics and Telecommunication Engineers, India)*, 34(4), 408–415. <https://doi.org/10.1080/02564602.2016.1196620>

18. Ray, P. K., Mohanty, A., & Panigrahi, T. (2019). Power quality analysis in solar PV integrated microgrid using independent component analysis and support vector machine. *Optik*, 180, 691–698. <https://doi.org/10.1016/j.ijleo.2018.11.041>
19. Rupal, H. S., Ankit, K. T., Mohanty, S. R., & Kishor, N. (2018). Detection and classification of power quality disturbances using signal processing techniques. *Asia-Pacific Power and Energy Engineering Conference, APPEEC, 2017-Novem*, 1–6. <https://doi.org/10.1109/APPEEC.2017.8308934>
20. Shen, Y., Hussain, F., Liu, H., & Addis, D. (2018). Power quality disturbances classification based on curvelet transform. *International Journal of Computers and Applications*, 40(4), 192–201. <https://doi.org/10.1080/1206212X.2017.1398213>
21. Singh, U., & Singh, S. N. (2019). A new optimal feature selection scheme for classification of power quality disturbances based on ant colony framework. *Applied Soft Computing Journal*, 74, 216–225. <https://doi.org/10.1016/j.asoc.2018.10.017>
22. Uyar, M., Yildirim, S., & Gencoglu, M. T. (2008). An effective wavelet-based feature extraction method for classification of power quality disturbance signals. *Electric Power Systems Research*, 78(10), 1747–1755. <https://doi.org/10.1016/j.epsr.2008.03.002>
23. Wang, S., & Chen, H. (2019). A novel deep learning method for the classification of power quality disturbances using deep convolutional neural network. *Applied Energy*, 235(March 2018), 1126–1140. <https://doi.org/10.1016/j.apenergy.2018.09.160>
24. Zhang, H., Liu, P., & Malik, O. P. (2003). Detection and classification of power quality disturbances in noisy conditions. *IEE Proceedings: Generation, Transmission and Distribution*, 150(5), 567–572. <https://doi.org/10.1049/ip-gtd:20030459>